

# Practical and robust experimental determination of $c_{13}$ and Thomsen parameter $\delta$

Fuyong Yan<sup>1\*</sup>, De-Hua Han<sup>1</sup> and Xue-Lian Chen<sup>2</sup>

<sup>1</sup>Rock Physics Laboratory, Department of Earth and Atmospheric Sciences, University of Houston, Houston, TX 77204 USA, and <sup>2</sup>School of Geosciences, China University of Petroleum, Qingdao 266580, China

Received August 2015, revision accepted February 2017

## ABSTRACT

We analysed the complications in laboratory velocity anisotropy measurement on shales. There exist significant uncertainties in the laboratory determination of  $c_{13}$  and Thomsen parameter  $\delta$ . These uncertainties are primarily related to the velocity measurement in the oblique direction. For reliable estimation of  $c_{13}$  and  $\delta$ , it is important that genuine phase velocity or group velocity be measured with minimum uncertainty. The uncertainties can be greatly reduced if redundant oblique velocities are measured. For industrial applications, it is impractical to make multiple oblique velocity measurements on multiple core plugs. We demonstrated that it is applicable to make multiple genuine oblique group velocity measurements on a single horizontal core plug. The measurement results show that shales can be classified as a typical transversely isotropic medium. There is a coupling relation between  $c_{44}$  and  $c_{13}$  in determining the directional dependence of the seismic velocities. The quasi-P-wave or quasi-S-wave velocities can be approximated by three elastic parameters.

**Key words:** Transverse isotropy, Thomsen parameters, Shale, Group velocity.

## INTRODUCTION

Muckrocks or shales make up about 75% of the sedimentary rocks in volume and are becoming important reservoir rocks for hydrocarbon resources. Shales are usually anisotropic in elastic properties. The anisotropic properties may have a significant effect on seismic imaging and seismic amplitude interpretations. Therefore, study of the physical properties of shales is important for seismic exploration. Laboratory velocity anisotropy measurements on shales are done routinely nowadays. Shales are often treated as transversely isotropic (TI) media. The measurement results are often reported in terms of Thomsen parameters (Vernik and Nur 1992; Johnston and Christensen 1995; Vernik and Liu 1997; Jakobsen and Johansen 2000; Sondergeld *et al.* 2000; Wang 2002a, b; Dewhurst and Siggins 2006; Sarout *et al.* 2007; Sarout and Guéguen 2008; Sondergeld and Rai 2011; Sone 2012; Sarout *et al.* 2014). Of the three parameters ( $\epsilon$ ,  $\gamma$ , and  $\delta$ ),  $\delta$  is the most

important parameter for exploration geophysicists because it describes the relation between normal moveout velocity and vertical velocity (Thomsen 1986; Tsvankin 2012). Thomsen (1986) pointed out that  $\delta$  is an “awkward” combination of elastic parameters, and its physical meaning is not straightforward. In spite of a large number of laboratory measurements, our understanding of the parameter is not clear (Banik 1987; Sayers 2004). Laboratory measurement results show that  $\delta$  has poor correlation with other Thomsen parameters, and even the normal data range of  $\delta$  for shales is not certain. Considering the challenges and uncertainties in laboratory velocity anisotropy measurements of shales, different setups for velocity anisotropy measurement have been brought up in recent years. To acquire all the TI anisotropy parameters, traditionally, the measurements are made on three core plugs (Vernik and Nur 1992; Vernik and Liu 1997; Sondergeld *et al.* 2000) orientated at 0°, 45°, and 90° with respect to the vertical direction. To improve the measurement efficiency, Jakobsen and Johansen (2000) attempted conducting velocity anisotropy measurement on a vertical core plug, and Wang (2002a)

\*E-mail: yanfyon@yahoo.com

designed a setup for velocity anisotropy on a horizontal core. Both setups tried to measure the oblique group velocity on the cylindrical walls of a core plug. Determining  $c_{13}$  and  $\delta$  is most sensitive to error in the oblique velocity measurement. The oblique velocity measured on the cylindrical wall may have more uncertainty because a flat piezoelectric transducer has a line contact with the cylindrical wall of the sample. If the measurement is made on the axial direction, the whole plane of the piezoelectric transducer can contact the end surface of the cylindrical sample.

Multiple oblique velocity measurements in different directions should significantly reduce the uncertainty in estimating of  $c_{13}$  and  $\delta$ . The velocity anisotropy measurements by Jakobsen and Johansen (2000) were based on 11 core plugs, and Sone's measurements (2012) were based on five core plugs. In practice, preparation of multiple core samples with accurate direction control from the same depth interval is a very time-consuming and thus expensive process. In actual velocity measurements, most of the time is spent on preparing the sample and putting the sample in and taking the sample out from the pressure vessel. These processes are the most error-prone. Another disadvantage of multiple core measurements is that they can introduce extra heterogeneities and complicate the result. Therefore, it is preferred that reliable velocity anisotropy measurements are conducted on a single core plug. Blum, Adam and van Wijk (2012, 2013) used laser technology to measure the elastic anisotropy based on a single horizontal core plug. In their measurement, no stress is applied to the horizontal core sample. The sample can be rotated freely for group velocity measurements at different angles. Although this technique is innovative, the first-arrival signal is not clear, and it is very challenging to build it into a pressure vessel. The estimated  $\delta$  values for the two samples under study are quite unusual (i.e.,  $-0.27$  for one shale sample and  $6.62$  for the other). Sarout *et al.* (2015) tried performing multiple oblique group velocity measurements on a vertical shale sample (the bedding direction is perpendicular to the axial direction of the cylindrical sample). They applied piezoelectric transducers of 6-mm diameter on a vertical core sample with a diameter of 38 mm. Their setup has advantage in simulating the *in situ* stress conditions, but it may be a challenge to measure the genuine group velocity because the principle of group velocity measurement is that the signal is emitted from a "point" source and received by a "point" receiver relative to the wave travel path.

In spite of a large amount of effort made on velocity anisotropy measurements of shales, the estimation of the critical anisotropic parameter  $\delta$  still needs significant

improvement. In this study, we will try to demonstrate that a reliable and efficient estimation of  $c_{13}$  and  $\delta$  can be made on a single horizontal core plug.

## GROUP VELOCITY AND PHASE VELOCITY MEASUREMENT

In an anisotropic medium, there exist differences in both magnitude and direction between the group velocity and the phase velocity. The group velocity, also called ray velocity, is the speed by which the energy travels. The phase velocity is the instantaneous wave travel speed directly related to the particle motion. It is always normal to the wavefront. The coupling relations between the group velocity and the phase velocity and between the group angle and the phase angle are given by (Byun 1984)

$$\tan(\varphi - \theta) = \frac{1}{V_\theta} \frac{dV_\theta}{d\theta}, \quad (1)$$

$$V_\theta = V_\varphi \cos(\varphi - \theta), \quad (2)$$

where  $\varphi$  and  $\theta$  refer to the group angle and the phase angle, respectively, when they are used as normal text. They denote the group velocity and the phase velocity, respectively, when they are used as subscripts. Velocity  $V$  can be for any of the three wave modes. Using laboratory-measured parameters of a shale sample by Vernik and Liu (1997), Fig. 1 illustrates the coupling relations between the group velocity and the phase velocity and between the group angle and the phase angle. The elastic parameters of this shale sample are given in the figure caption. It can be seen that the relative difference between the group angle and the phase angle may be greater than the scalar difference between the group velocity and the phase velocity. Deviation of the group velocity from the phase velocity is controlled by the anisotropic properties and the direction of wave propagation. The deviation patterns are quite different for the quasi-P-wave and SV-wave. The direction difference can be more than  $20^\circ$  for some strongly anisotropic shales.

Confusions of the group-phase concepts can introduce significant error in velocity anisotropy measurements. For the shale sample used for illustration in Fig. 1, the estimated  $c_{13}$  is 6.58 GPa, and the Thomsen parameter  $\delta$  is 0.03. If  $45^\circ$  group velocity is mistaken for  $45^\circ$  phase velocity and the non-oblique velocities are kept unchanged, then the estimated  $c_{13}$  will be  $-0.38$  GPa and the Thomsen parameter  $\delta$  will be  $-0.25$ . For a transversely isotropic (TI) medium, the three principal

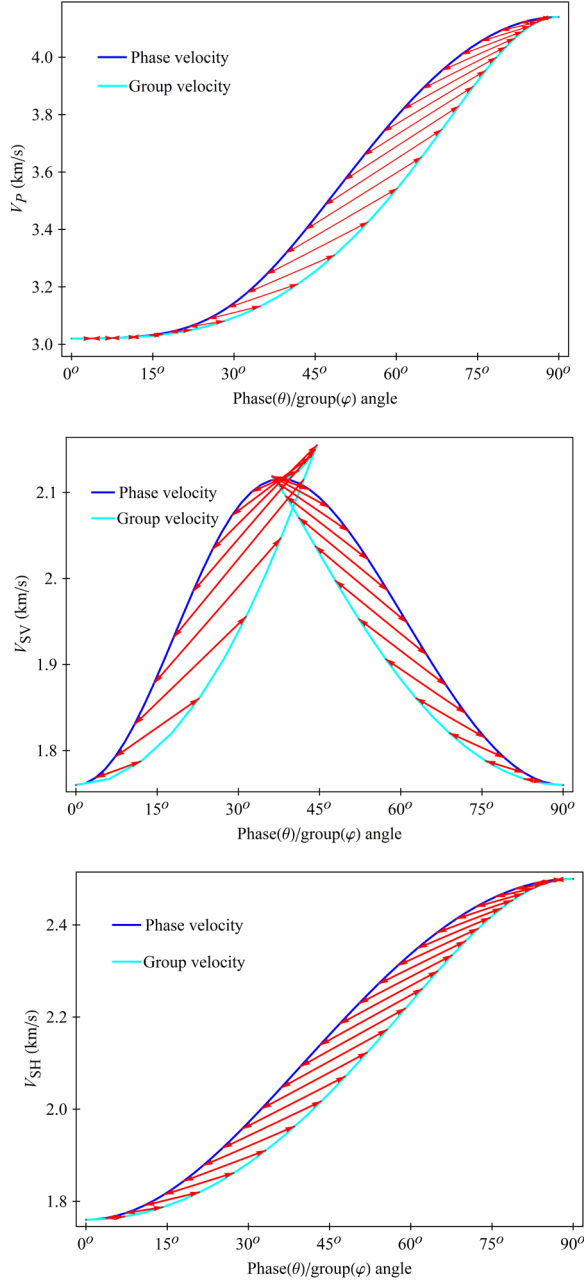


**Figure 1** Coupling relations between phase velocity and group velocity and phase angle and group angle. The double arrow connects phase velocity at a certain phase angle and its corresponding group velocity in a certain group angle. The plot is based on Bakken shale sample at 2632 m (Vernik and Liu 1997), with parameters:  $c_{11} = 35.31$  GPa,  $c_{33} = 18.79$  GPa,  $c_{44} = 6.38$  GPa,  $c_{66} = 12.87$  GPa,  $c_{13} = 6.58$  GPa, and  $\rho = 2.06$  g/cc.

Poisson's ratios are defined by the TI elastic constants as (King 1964; Yan *et al.* 2016)

$$v_V = \frac{c_{13}}{2(c_{11} - c_{66})} \quad (= v_{31} = v_{32}), \quad (3)$$

$$v_{HV} = \frac{2c_{13}c_{66}}{c_{11}c_{33} - c_{13}^2} \quad (= v_{13} = v_{23}), \quad (4)$$

$$v_{HH} = \frac{c_{33}(c_{11} - 2c_{66}) - c_{13}^2}{c_{11}c_{33} - c_{13}^2} \quad (= v_{12} = v_{21}). \quad (5)$$

The dynamic principal Poisson's ratios ( $v_V$ ,  $v_{HV}$ , and  $v_{HH}$ ) will change to  $-0.01$ ,  $-0.01$ , and  $0.27$  from their original values  $0.15$ ,  $0.27$ , and  $0.22$ , respectively, if the  $45^\circ$  group velocity is mistaken as the  $45^\circ$  phase velocity. For this sample, the scalar difference between the  $45^\circ$  group velocity and the  $45^\circ$  phase velocity is about 6%. This difference can cause significant error in estimating  $c_{13}$  and  $\delta$  and lead to erroneous interpretation of the deformation behaviour of the TI medium. Yan, Han and Yao (2012) showed that 1% error in estimating of  $45^\circ$  P-wave phase velocity can cause significant error in estimating  $c_{13}$  and  $\delta$ . Therefore, for reliable estimation of  $c_{13}$  and  $\delta$ , maximum effort should be made to ensure that genuine phase velocity or group velocity is measured with minimum uncertainty.

The five elastic constants defining a TI medium can be obtained from five velocity measurements as follows:

$$c_{11} = \rho V_{P90^\circ}^2, \quad (6)$$

$$c_{33} = \rho V_{P0^\circ}^2, \quad (7)$$

$$c_{44} = \rho V_{SH0^\circ}^2 = \rho V_{SV0^\circ}^2 = \rho V_{SV90^\circ}^2, \quad (8)$$

$$c_{66} = \rho V_{SH90^\circ}^2, \quad (9)$$

$$c_{13} = \sqrt{(2\rho V_{P45^\circ}^2 - c_{11} - c_{44})(2\rho V_{P45^\circ}^2 - c_{33} - c_{44})} - c_{44}, \quad (10)$$

where the subscripts P, SV, and SH denote three wave modes, respectively, and subscript  $\theta$  denotes the phase velocity or phase angle. The angle is relative to the TI symmetry axis.  $V_{P45^\circ}$  is the  $45^\circ$  P-wave phase velocity.

Estimation of  $c_{11}$ ,  $c_{33}$ ,  $c_{44}$ , and  $c_{66}$  is straightforward. They can be determined from traditional ultrasonic velocity measurement in the non-oblique directions, and usually, there should be no extra uncertainties introduced. For a TI medium, the group velocity is identical to the phase velocity

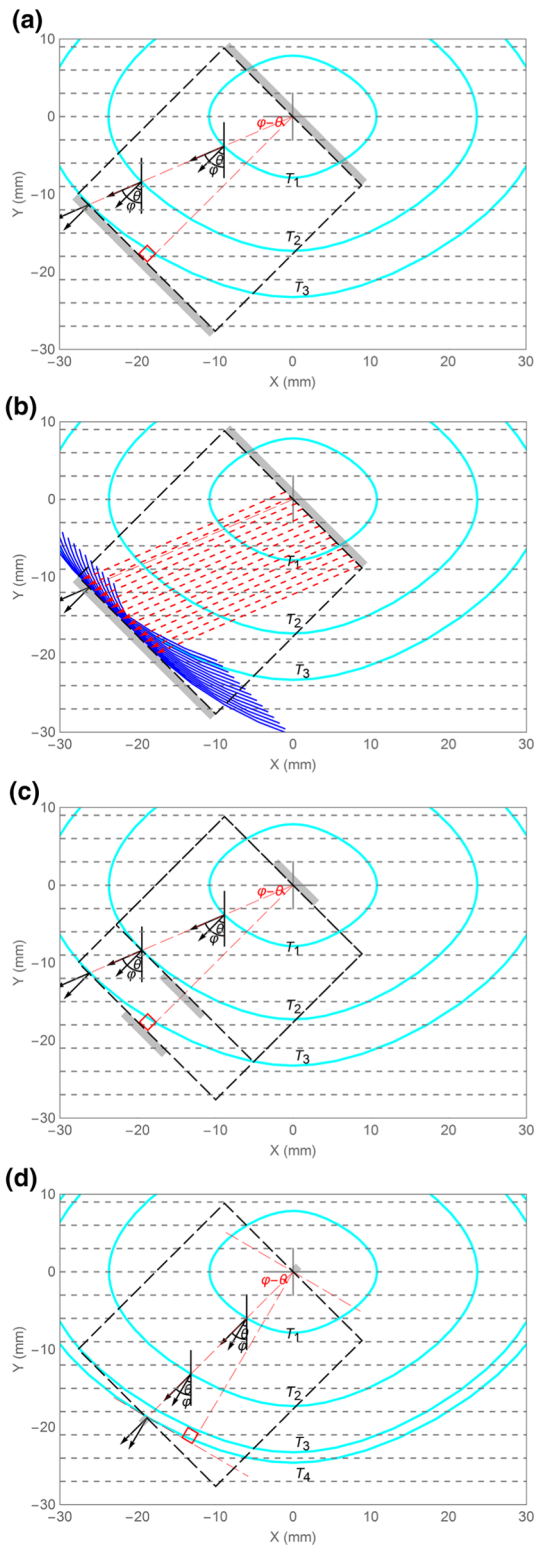


**Figure 2** Wavefront propagation modelling for quasi-P-wave velocity measurement on a 45° plug. The grey bars represent the piezoelectric transducers. The cyan curves are the wavefronts at different times

in the non-oblique directions. After  $c_{11}$ ,  $c_{33}$ , and  $c_{44}$  are determined, a velocity must be measured in an oblique direction to estimate  $c_{13}$ . The oblique P-wave instead of SV-wave is usually utilised to estimate  $c_{13}$  because there might be converted P-wave signals before the SV-wave signal arrives, and possible triplication around 45° will make first break time picking on the SV-wave signal more difficult. The oblique P-wave velocity is usually made on a 45° plug (Vernik and Nur 1992). It can be seen from equation (10) that  $c_{13}$  is most sensitive to the measurement error of this oblique velocity. The phase angle does not necessarily have to be 45°. If the phase angle is not 45°,  $c_{13}$  can be estimated by (Yan *et al.* 2016)

$$c_{13} = 2 \csc 2\theta \sqrt{(\rho V_{p0}^2 - c_{11} \sin^2 \theta - c_{44} \cos^2 \theta)(\rho V_{p0}^2 - c_{33} \cos^2 \theta - c_{44} \sin^2 \theta) - c_{44}} \quad (11)$$

Compared to the measurement error in the numerical value, a more important issue associated with the oblique velocity measurement is what type of velocity is actually estimated. Yan *et al.* (2016) discussed that the oblique velocity measurement made on a horizontal plug (Wang 2002a) is not a phase velocity, and Wang's data (2002b) need correcting for mistaking group velocity as phase velocity. If we are not sure whether group velocity or phase velocity is measured, errors may be made in both the scalar magnitude of the velocity and the propagation direction. Fig. 2 shows the wavefront propagation simulations of the oblique velocity measurements on a 45° core plug. The dashed rectangle denotes the cross section of the sample passing the cylindrical axis. The grey dashed lines denote the bedding direction of the TI medium. The diameter of the sample is 25.0 mm, and the sample length is 26.5 mm. The grey bars represent the disk-shaped P-wave piezoelectric transducers. The cyan curves are the wavefronts

issued from the centre of the transmit transducer. The grey dash lines show the bedding direction, and the black dashed rectangle or circle denotes the cross section of the cylindrical sample. The TI medium has same properties as the medium used in Fig. 2. (a) The transducers covering the whole end surfaces of the cylindrical sample and only wavefronts from one source are shown. (b) The transducers covering the whole end surfaces of the cylindrical sample are shown. The wavefronts from multiple sources demonstrate propagation of a deviated plane wave. (c) The transducers have a diameter of 7.5 mm. Genuine phase velocity measurement is affected by both the transducer dimension and sample length. (d) The transducers have a diameter of 1.4 mm. When the transducer can be approximated as a point source relative to the wave propagation path, group velocity is measured.

of P-wave at different times issued from the centre of the emission transducer. The solid arrows denote the ray direction, and the dashed arrows denote the phase direction. In panel (a), when the wavefront reaches the interface between the receiver transducer and the end surface of the sample at time  $T_3$ , the wavefront is tangential to this interface. At the tangential point, the particle motion, which is the phase velocity direction, is parallel to the normal direction of the interface. It is parallel to the axial direction of the sample. The P-wave phase velocity at  $45^\circ$  is obtained by dividing the sample length by the travel time  $T_3$ . As demonstrated in panel (b), on a  $45^\circ$  plug, we are actually trying to measure the travel speed of a deviated plane wave. Based on Huygens–Fresnel principle, each point of the plane wave at the interface between the emission transducer and the sample can be treated as new point sources. The wavefronts from these point sources overlay at the interface between the sample and the receiver transducer and form a plane wavefront. At this interface, the deviation of the plane wave off the axial direction of the sample is determined by

$$\Delta x = L \tan(\varphi - \theta), \quad (12)$$

where  $L$  is the sample length. The angle difference  $\varphi - \theta$  is determined by the TI elastic properties of the measured sample and orientation of the sample. The deviation  $\Delta x$  is proportional to the sample length. In practice, for reliable first break time picking, the transducer should be wide enough so that at least 10% of the wavefront of the deviated plane wave can arrive simultaneously on the receiver transducer (Dellinger and Vernik 1994). Panel (c) shows the effect of the transducer dimension and sample length on genuine phase velocity measurement. For clarity, only wavefronts emitted from the centre of the emission transducer are shown. The diameter of the transducers is 7.5 mm. When the sample is 26.5 mm long, the setup will have a problem in estimating the genuine phase velocity because the first-arrival time on the receiver transducer will be later than time  $T_3$ . A longer sample requires a transducer of greater dimensions, but the size of the transducer is limited by the measurement design. If the wavefront of the deviated plane wave is missed by the receiver transducer, the first-arrival time related to the phase velocity will be overestimated and the velocity be underestimated. Traditionally, a greater sample length is thought to be beneficial for accurate velocity measurement. Therefore, there could be a bias toward underestimation of the phase velocity measured on a  $45^\circ$  plug. From equation (10), underestimation of the oblique phase velocity leads to underestimation of  $c_{13}$ . When the transducer can be treated as a point source relative to the

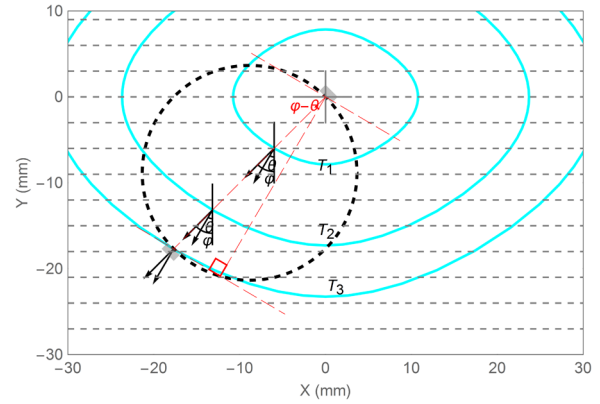
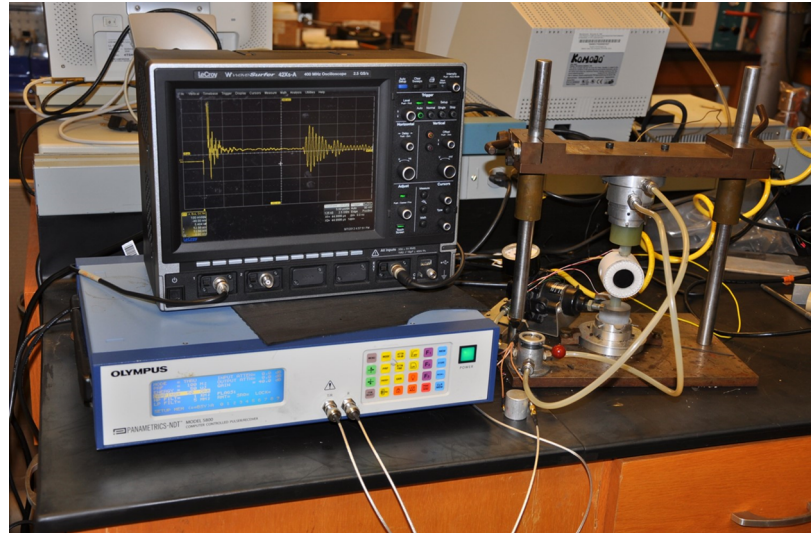


**Figure 3** Wavefront propagation modelling for quasi-P-wave velocity measurement on a horizontal. The grey bars represent the piezoelectric transducers. The cyan curves are the wavefronts at different times issued from the centre of the transmit transducer. The grey dash lines show the bedding direction, and the black dashed rectangle or circle denotes the cross section of the cylindrical sample. The TI medium has same properties as the medium used in Fig. 2. In Figs. 2 and 3,  $T_1$ ,  $T_2$ ,  $T_3$ , and  $T_4$  represent travel times of 2.60, 5.72, 7.70, and 8.14  $\mu\text{s}$ , respectively.

wave travel path, as shown in panel (d), the measured velocity should be close to group velocity.

Figure 3 shows wavefront propagation modelling for the oblique velocity measurement on a horizontal core plug. The dashed disk represents the radial cross section of a horizontal shale sample with a diameter of 25.0 mm. The grey bars represent the P-wave piezoelectric transducers. The cyan curves are the wavefronts at different times issued from the centre of the transmit transducer. The basic principle for group velocity measurement is “point source to point receiver” in the sagittal plane passing the TI symmetry axis. The transducer has a point contact with the cylindrical surface of a horizontal plug in cross section and a line contact in a 3D sense. We use the diameter of the sample to divide the travel time, allowing the group velocity to be estimated. The distance travelled by the compressional wave in the corresponding phase direction is represented by the longer leg of the right triangle in red. This distance is not known before the TI elastic properties of the shale sample are estimated. For the oblique velocity measurement on a horizontal plug, if the contacting line between the flat transducer and the cylindrical wall is decomposed into numerous point sources, signals emitted from the sources will arrive on the receiver transducer simultaneously. The transducer does not need to be small enough as a “point” relative to the diameter of the sample as long as the contact between the transducer to the cylindrical wall is

Figure 4 Benchtop rotational group velocity measurement setup.



close to a “point” in the cross section, as shown in Fig. 3. For the oblique velocity measurement on a vertical plug, if the contacting line between the flat transducer and the cylindrical wall is decomposed into numerous point sources, the signal emitted from the point with the shortest distance to the proximal edge of the receiver transducer will be the earliest to be received. The signals from other points of the line source will be received subsequently at different times. The first-arrival signal is thus geometrically dispersed. To measure the genuine group velocity, the transducer needs to be small enough as a “point” relative to the wave travel path. If the transducer is too small, the wave signal might be too weak for reliable velocity estimation. Therefore, it is more advantageous to measure real group velocity on a horizontal plug than on a vertical plug.

## EXPERIMENTAL SETUP AND METHOD

As we analysed earlier, there are significant uncertainties in the estimation of  $c_{13}$  and Thomsen parameter  $\delta$ . The uncertainties are primarily related to the oblique velocity measurement and can be greatly reduced if multiple oblique velocities are measured. One feasible way to obtain a large amount of reliable laboratory velocity anisotropy measurement data for industrial applications is to make multiple oblique velocity measurements on a single horizontal core plug. The oblique velocities measured on the radial directions of a horizontal core plug are group velocities.

Figures 4 and 5 show the laboratory setup for rotational group velocity measurements. A uniaxial stress of about

300 psi is applied to the shale sample for good coupling between the transducer buffers and the shale sample. The stress can be easily applied and released by letting the compressed air in or out of the gas chamber located below the beam of the benchtop. After releasing the stress, the core samples can be rotated to the next direction for the next oblique velocity measurement. In order to acquire the true group velocity, the end surfaces of the transducer buffers should be flat so that rays are forced to go diametrically across the sample from one point to the other point in the cross section. In a 3D sense, the horizontal core plug has a line contact with the transducer buffers, so the first break signal can be strong enough for accurate travel-time picking. The central frequency of the P-wave piezoelectric transducer we used is about 1 MHz.

The multiple P-wave oblique velocity measurements cannot acquire all the transversely isotropic (TI) elastic constants. The ultrasonic velocity measurement on a cylindrical sample is usually conducted on the axial direction because the coupling between the transducer and the end surface of the sample is much better than the coupling in the radial direction. Three velocities ( $V_{P90^\circ}$ ,  $V_{SV90^\circ}$ , and  $V_{SH90^\circ}$ ) can be measured on a cylindrical horizontal shale sample. We did not repeat the measurement on the axial direction because the samples under study were first measured for velocity anisotropy half a year ago on our five-component ( $V_{P0^\circ}$ ,  $V_{P90^\circ}$ ,  $V_{SV90^\circ}$ ,  $V_{SH90^\circ}$ , and  $V_{P\psi45^\circ}$ ), single-horizontal-plug velocity anisotropy measurement system (Wang 2002a; Yan *et al.* 2012). The earlier measurements are primarily used for comparative study. Only the information of  $V_{SV90^\circ}$  is used in the estimation of  $c_{13}$  and  $\delta$ . In both measurements, no attempts were made to change

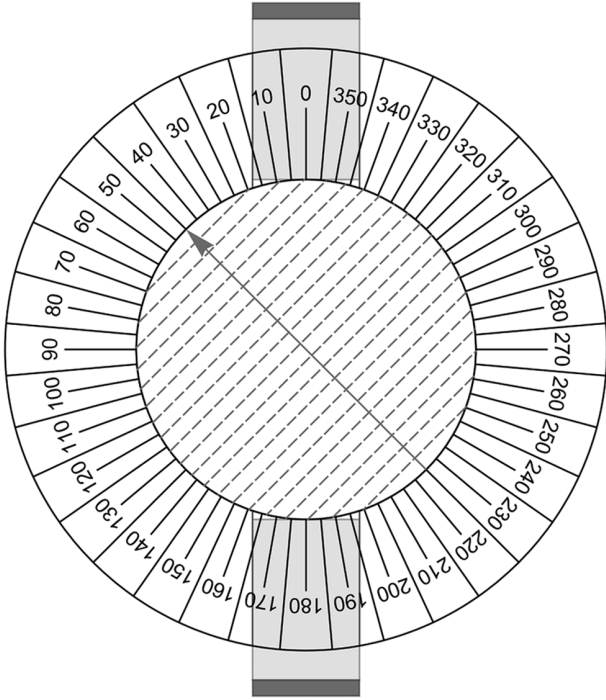


**Figure 5** Diagram of rotational group velocity measurement. Inside the Phenolite tube pinned with an angle panel is a horizontal plug, with the dashed lines denoting the bedding direction. The TI symmetric axis is marked on the sample, and the arrow points to the group angle. The dark grey rectangles represent the piezoelectric transducers, and the light grey rectangles represent the buffers.

the pore fluid composition, and the pore pressure is the atmospheric pressure.

After the TI elastic constants are determined, the Thomsen parameters (Thomsen 1986) can be calculated by

$$\delta = \frac{(c_{13} + c_{44})^2 - (c_{33} - c_{44})^2}{2c_{33}(c_{33} - c_{44})}, \quad (13)$$

$$\varepsilon = \frac{c_{11} - c_{33}}{2c_{33}}, \quad (14)$$

$$\gamma = \frac{c_{66} - c_{44}}{2c_{44}}. \quad (15)$$

## MEASUREMENT RESULTS

We made rotational group velocity measurements on two Haynesville Shale samples: sample A and sample B. Figure 6 shows the P-wave signal traces at directions from  $0^\circ$  to  $180^\circ$  with respect to the transversely isotropic symmetry axis, increasing at a  $10^\circ$  interval, for shale sample A. The P-wave

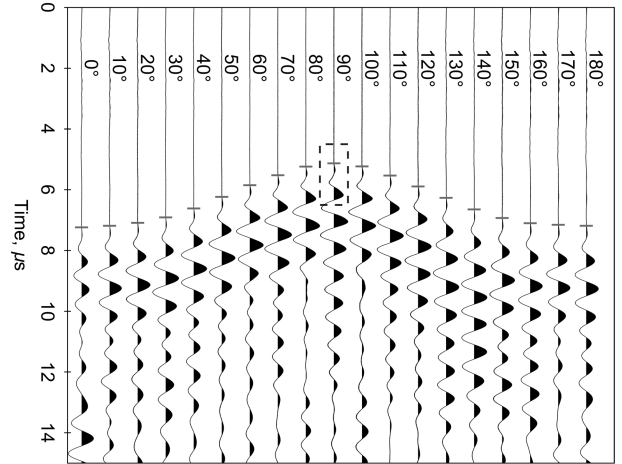


**Figure 6** P-wave signal traces at different directions with respect to the TI symmetric axis. The first-arrival signal in the dashed rectangle on the trace measured at  $90^\circ$  is magnified and shown in Fig. 7.

signal at  $90^\circ$  (parallel to the bedding) is the usually strongest and clearest compared with the P-wave signals at other directions. For comparison, the maximum amplitude of the each trace is normalised to one. Due to the limited contact area between the buffers and the sample, the first break signal is very weak relative to the later coming signals, but the sequential time variation of the received signals is obvious and in a clear trend, as shown in Fig. 6. The signal around the first break time marked by the dashed rectangle on the trace at  $90^\circ$  is shown in Fig. 7. It is shown that the first-arrival P-wave signals are strong enough for confident first break time picking. The buffer time was deducted from the time axis. The recorded waveform has a time sampling rate of 2 GS/s.

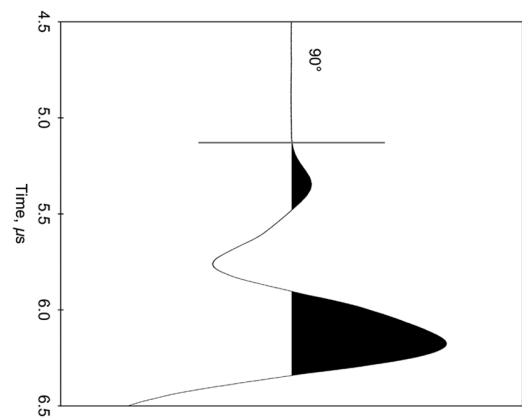


**Figure 7** Magnification of the P-wave first-arrival signal measured at  $90^\circ$ . The first break time may be not clear in Fig. 6. It can be picked with confidence after magnification.

The error in first break time picking is less than  $0.05 \mu\text{s}$ . The absolute velocity error caused by time picking can be controlled by less than 1%. By comparing and matching the first-arrival waveforms between different traces, the relative velocity error between different directions should be much smaller than the absolute velocity error. The short bar on each trace shows the first break time we picked.

Figure 8 shows the estimated P-wave group velocities from two independent velocity anisotropy measurement systems for sample A. The data points marked by triangles are estimated from the five-component single-horizontal-plug velocity anisotropy measurement system. The different data points at the same angle are from different pressure conditions (at differential pressures from 1000 to 5000 psi). The differential pressure refers to the pressure difference between the confining pressure and the pore pressure. The unfilled squares with error bars are from benchtop rotational group velocity measurements. In spite of different stress conditions, the two independent sets of measurements are generally consistent. For this sample, the stress effect on velocity is much smaller than the directional dependence.

### TRANSVERSELY ISOTROPIC ELASTIC CONSTANT INVERSION AND SENSITIVITY ANALYSIS

For a transversely isotropic (TI) medium, the quasi-P-wave phase velocity is a function of the phase angle and four elastic constants ( $c_{11}$ ,  $c_{33}$ ,  $c_{44}$  and  $c_{13}$ )

$$V_{P\theta} = \sqrt{\frac{(c_{11}\sin^2\theta + c_{33}\cos^2\theta + c_{44} + \sqrt{M})}{2\rho}}, \quad (16)$$

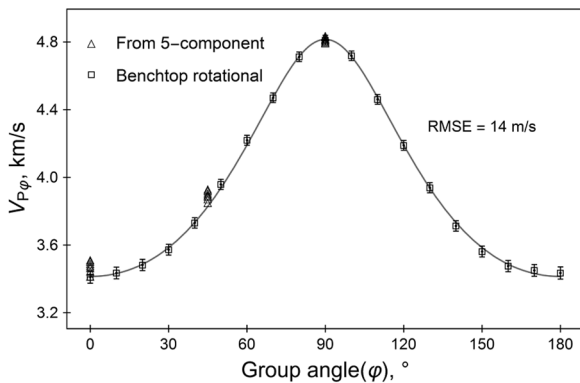


Figure 8 Measured group velocities at different directions with respect to the TI symmetrical axes for sample A. The curve shows the least squares fitting of the measured data using the TI theory.

where

$$M = [(c_{11} - c_{44})\sin^2\theta - (c_{33} - c_{44})\cos^2\theta]^2 + (c_{13} + c_{44})^2\sin^2(2\theta).$$

From equations (1), (2), and (16), the group velocity is an implicit function of group angle and four elastic constants

$$V_{P\phi} = F(\phi, c_{11}, c_{33}, c_{44}, c_{13}). \quad (17)$$

From this implicit relation, the least squares regression technique is utilised to find the four elastic constants that can minimise the summation of the squared errors

$$S = \sum_{i=1}^N (V_{P\phi data} - V_{P\phi})^2, \quad (18)$$

where  $N$  is the number of oblique velocities measured in different radial directions. We should be able to invert for the four elastic constants by least squares fitting because group velocities at 19 different group angles were acquired. In practice, we found that the inversion results for  $c_{44}$  and  $c_{13}$  are totally dependent on the initial input values. From sensitivity analysis, we found that there is a coupling relation between  $c_{44}$  and  $c_{13}$ . In Fig. 9,  $c_{11}$  and  $c_{33}$  are kept constant (58.38 and 29.52 GPa, respectively) for all the curves. For each value of  $c_{44}$  that is sequentially changed from 3, 6, 9, 12, and 15 to 18 GPa, a value of  $c_{13}$  can always be found to match the measured group velocity variation trend visually. Considering the measurement uncertainties, no matter how many oblique quasi-P-wave velocities are measured, it is impossible to simultaneously determine the four elastic constants.

For sake of clarity, we make a further attempt to use the phase velocity, i.e., equation (16), to demonstrate the coupling relation between  $c_{44}$  and  $c_{13}$  because the relationship between the group velocity and the four TI elastic constants is not explicit. In Fig. 10, we made a similar sensitivity analysis based on velocity anisotropy measurement data of a Bakken shale sample from Vernik and Liu (1997). The black curve shows the phase velocity based on the laboratory measurements.  $c_{11}$  and  $c_{33}$  are kept constant, and  $c_{44}$  is varied sequentially from 5, 7, 9, 11, and 13 to 15 GPa. For each  $c_{44}$  value, using the hit-and-miss method, we can always find a value for  $c_{13}$  that can approximately match the phase velocity curve based on laboratory measurements. Although the  $c_{44}$ - $c_{13}$  pairs are drastically different, the phase velocity curves almost overlay with each other. The curves can only be differentiated with each other after significant magnification, as displayed by the inserted plot. The velocity difference is beyond resolution of

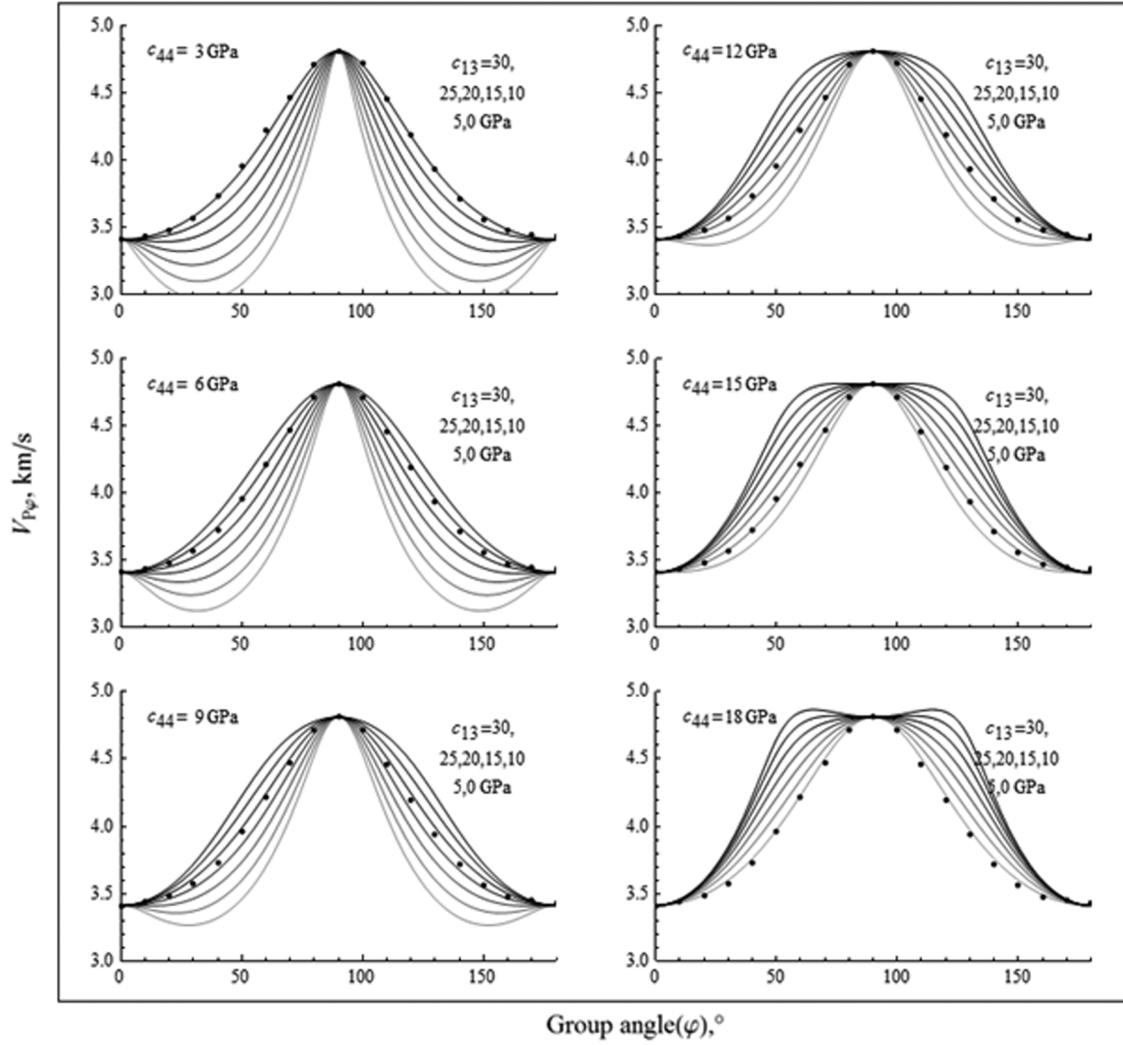


**Figure 9** Coupling relation between  $c_{44}$  and  $c_{13}$  in matching the measured group velocity trend: Let  $c_{11}$  and  $c_{33}$  be constants;  $c_{44}$  and  $c_{13}$  are sequentially changed to find possible combinations of  $c_{44}$  and  $c_{13}$  matching the measured group velocity trend.

common laboratory ultrasonic velocity measurements on core samples. Therefore,  $c_{44}$  and  $c_{13}$  are practically impossible to be estimated from multiple oblique velocity measurements. Although the selected  $c_{44}$  and  $c_{13}$  can have quite different values from the measured values, the estimated values of  $\delta$  are close to the true value as long as the phase velocity curve fits with that based on laboratory measurements.

From the above analysis, for practical applications, the directional dependence of the quasi-P-wave in a TI medium can be sufficiently described by three elastic parameters ( $V_{p0^\circ}$ ,  $V_{p90^\circ}$ , and  $\delta$ ), instead of four elastic parameters, as shown in equation (16). Our observation complies with the theoretical foundation of velocity analysis in TI media (Tsvankin and Thomsen 1994; Alkhalifah and Tsvankin 1995; Tsvankin

2012). For a layer of TI medium with arbitrary anisotropy, the P-wave reflection travel time can be approximated by

$$t^2 = t_0^2 + \frac{x^2}{V_{\text{PNMO}}^2} - \frac{(V_{p90^\circ}^2 - V_{\text{PNMO}}^2)x^4}{V_{\text{PNMO}}^2(t_0^2 V_{\text{PNMO}}^4 + V_{p90^\circ}^2 x^2)}, \quad (19)$$

where  $t_0$  is the two-way travel time in the vertical direction and

$$V_{\text{PNMO}} = V_{p0^\circ} \sqrt{1 + 2\delta}. \quad (20)$$

In the derivation of equation (19), it is assumed that the vertical shear wave velocity is zero (Alkhalifah and Tsvankin 1995; Tsvankin 1996; Alkhalifah 1998). From our analysis, even if an incorrect value of zero is assigned to the vertical

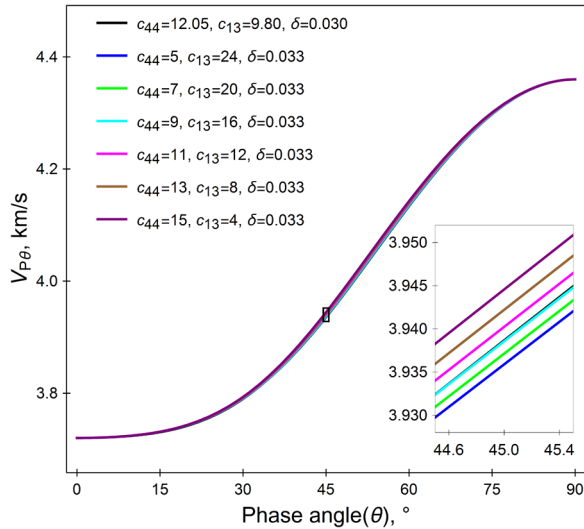


**Figure 10** Coupling effect of  $c_{44}$  and  $c_{13}$  on  $\delta$  from phase velocity matching. The black curve has the following properties:  $c_{11} = 45.24$  GPa,  $c_{33} = 29.94$  GPa,  $c_{44} = 12.05$  GPa,  $c_{13} = 9.80$  GPa, and  $\rho = 2.38$  g/cc (Vernik and Liu 1997). This sample comes from a depth of 11246 feet. Other curves have same  $c_{11}$  and  $c_{33}$  values and different  $c_{44}$  and  $c_{13}$  values.

shear wave velocity or  $c_{44}$ , a correct value of  $\delta$  can still be obtained. The normal moveout behaviour of the reflection travel time is actually controlled by three elastic parameters:  $V_{P0^\circ}$ ,  $V_{P90^\circ}$ , and  $\delta$ .

Although we cannot estimate  $c_{44}$  and  $c_{13}$  simultaneously from multiple oblique velocity measurements,  $c_{44}$  can be estimated independently from the slow shear wave velocity measurement in the axial direction (i.e., from  $V_{SV90^\circ}$ ). For this study,  $c_{44}$  is known from previous measurements (at a differential pressure of 1000 psi) on a five-component single-horizontal-plug velocity anisotropy measurement system. We can estimate  $c_{11}$ ,  $c_{33}$ , and  $c_{13}$  simultaneously by fitting the measured group velocity data using equations (17) and (18). As shown in Fig. 8, the theoretical curve fits the group velocity data almost perfectly. The estimated  $\varepsilon$  is 0.50, and  $\delta$  is 0.25 from the rotational group velocity measurements, which are close to the results from the previous measurement on the five-component single-horizontal-plug velocity anisotropy measurement system ( $\varepsilon = 0.49$ ,  $\gamma = 0.30$  at  $P_d = 1000$  psi). From the above sensitivity analysis, if we arbitrarily give  $c_{44}$  a value, using least squares fitting, we might not obtain the correct value for  $c_{13}$ , but the estimated  $\varepsilon$  and  $\delta$  should almost be same as the case when the true value of  $c_{44}$  is given. The high-degree of fitting demonstrates that shales can be classified as a typical TI medium.

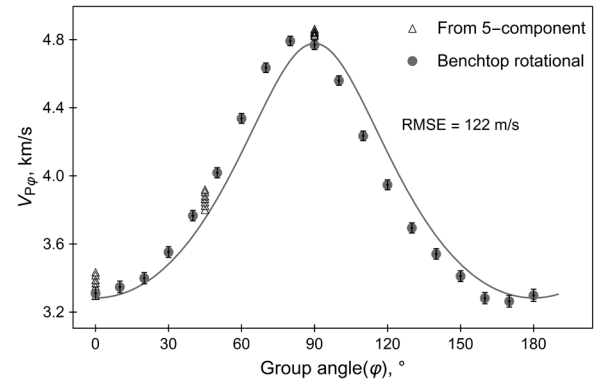


**Figure 11** Estimation of  $c_{11}$ ,  $c_{33}$ , and  $c_{13}$  by least squares fitting of the group velocity trend for shale sample B ( $c_{44}$  is taken from the five-component single-horizontal-plug velocity measurement at a differential pressure ( $P_d$ ) of 1000 psi).

## ANGLE ERROR DETECTION

In practical laboratory measurements, it is not always straightforward to identify the bedding direction of the shale sample. If the bedding direction is not correctly marked, all the subsequent velocity measurements are wrong. Sometimes, we can discover this error because the measured data may be inconsistent and do the measurement again with a corrected reference direction. Sometimes, the angle error might not be noticed. In Fig. 11, we plot the rotational group velocity measurement data together with the measurement results from the five-component single-horizontal-plug velocity anisotropy measurement system for shale sample B. From the rotational group velocity measurements, we noticed that the group velocity at  $80^\circ$  is slightly higher than the group velocity at  $90^\circ$ , and the group velocity at  $170^\circ$  is slightly lower than the group velocity at  $180^\circ$ . This is a good indication that there may be a significant error in identifying the bedding direction. As a result, the transversely isotropic (TI) theory cannot fit the measured group velocity trend with satisfaction.

The assumed TI symmetric direction marked on the end surface of sample B was re-examined. As shown in Fig. 12, it is indeed very difficult to tell the bedding direction by a visual check, and the double arrowed black line was originally identified as the direction perpendicular to the bedding. The visible crack only cuts through the edge of the sample and does not extend to the section where oblique velocities are actually measured. It should have little effect on the measured oblique velocities. By careful observation from different viewpoints, we realised that, quite possibly, we made an error in

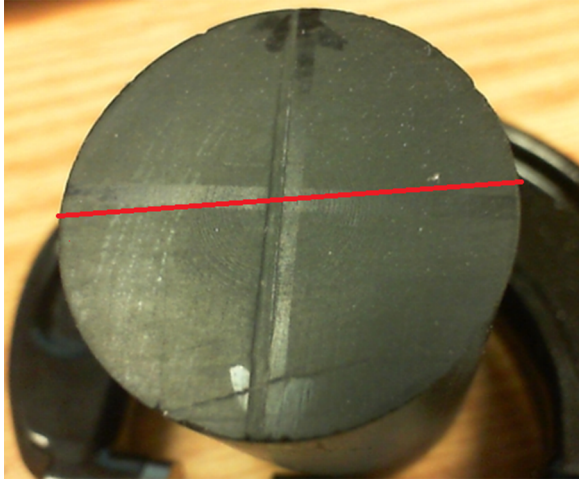


**Figure 12** Uncertainty in identification of the bedding direction on shale sample B (1-inch diameter). The double arrow marks the originally determined direction perpendicular to the bedding.

identifying the bedding direction. The red line may be a better judgment of the bedding direction. Considering the possible angle error, we added a variable  $\Delta\varphi$ , the group angle correction, in the least squares fitting. As shown in Fig. 13, after angle correction, the measured group velocity data can be fitted with the TI theory much better, and the root-mean-square error decreases from 122 to 16 m/s. The estimated  $\Delta\varphi$  is  $6.3^\circ$ . The velocity data from the five-component single-horizontal-plug velocity anisotropy system are also based on the wrong bedding direction, but only  $V_{p0^\circ}$  and  $V_{p\varphi 45^\circ}$  are needed to be

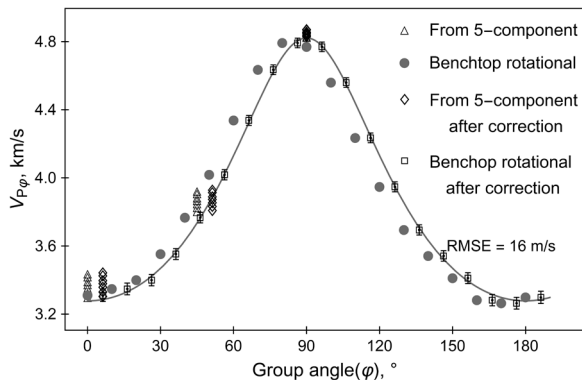


**Figure 13** Estimation of  $c_{11}$ ,  $c_{33}$ ,  $c_{13}$ , and  $\Delta\varphi$  by least squares fitting of the group velocity trend for shale sample B ( $c_{44}$  is taken from the five-component single-horizontal-plug velocity measurement at a differential pressure of 1000 psi). Except the velocities measured at the axial direction, all other velocities measured at radial directions are shifted by  $6.3^\circ$ , which is determined by least squares fitting using the TI theory.

shifted by the angle correction.  $V_{p90^\circ}$  is not shifted because it is measured on the axial direction of the horizontal plug. The Thomsen parameter  $\delta$  estimated from the five-component single-horizontal-plug velocity anisotropy system is 0.44; it is 0.36 from the rotational group velocity measurements and 0.33 after angle correction. The angle error does not cause significant difference in the estimation of  $\delta$  for this sample, but as shown by Yan *et al.* (2012), a  $5^\circ$  angle error can cause greater error in  $c_{13}$  and  $\delta$  in some cases. Identification and correction of possible angle error is another important reason that justifies the necessity for multiple oblique velocity measurements.

## DISCUSSION

As shown in Figs. 6 and 7, the first-arrival signals in the rotational group velocity measurements are very weak relative to the late-arriving signals. The P-wave transducers are made of economical piezoelectric ceramic disks with a central frequency of 1 MHz. They are stuck to PEEK buffers, without any damping material or design to improve the quality of the first-arrival signal. If the transducers are commercially made, the quality of the first-arrival signal can be significantly improved. The stress condition of the rotational group velocity measurement on the benchtop is far from that *in situ*. If the shale sample has visible cracks along the bedding, the wave signal in the direction perpendicular to the bedding may be too weak for first break time picking, and the sample can easily be broken under uniaxial stress of hundreds of psi. It is preferred that the multiple oblique velocity measurement unit be built into a pressure vessel. It is too expensive and technically challenging to build a rotating mechanism into the pressure vessel. A practical way is to add more P-wave transmission–receiver pairs on the jacket in radial directions based on the five-component single-horizontal-plug velocity anisotropy measurement setup (Wang 2002a). Limited by the circumference of the core plug or jacket, the P-wave transmission–receiver pairs can be separated into three groups located on different positions along the axial direction of the sample or jacket. Each group can have three or four pairs of P-wave transmission–receiver pairs in the radial cross section, and therefore, 9 or 12 P-wave velocities can be measured in different directions with respect to the TI symmetry axis. It should be noted that this system is limited to velocity anisotropy measurements under hydrostatic stress conditions. The measurement results might not directly apply to the subsurface scenarios when the vertical stress is not equal to the horizontal stresses.

## CONCLUSIONS

The rotational group velocity measurement results show that shales can be classified as a typical transversely isotropic (TI) medium in terms of elastic properties. It is feasible and necessary to make multiple oblique P-wave velocity measurements on a single horizontal core plug to reduce the uncertainty in estimating  $c_{13}$  and Thomsen parameter  $\delta$ . There is a coupling relation between  $c_{44}$  and  $c_{13}$  on the directional dependence of the seismic velocities in TI hydrocarbon source rocks. The coupling relation confirms the theoretical soundness of estimating the anisotropy parameters from seismic data using the velocity analysis technique.

## ACKNOWLEDGEMENTS

This study is sponsored by the Fluids/DHI Consortium of Colorado School of Mines and the University of Houston. Special thanks are given to Joel Sarout for his critical review and many constructive suggestions. The authors would like to thank two anonymous reviewers for their generous help in improving this paper.

## REFERENCES

- Alkhalifah T. 1998. Acoustic approximations for processing in transversely isotropic media. *Geophysics* **63**, 623–631.
- Alkhalifah T. and Tsvankin I. 1995. Velocity analysis for transversely isotropic media. *Geophysics* **60**, 1550–1566.
- Banik N.C. 1987. An effective anisotropy parameter in transversely isotropic media. *Geophysics* **52**, 1654–1664.
- Blum T.E., Adam L. and van Wijk K. 2012. Laboratory measurement of P-wave anisotropy in shales with laser ultrasonics. *SEG Expanded Abstracts*.
- Blum T.E., Adam L. and van Wijk K. 2013. Noncontacting benchtop measurements of the elastic properties of shales. *Geophysics* **78**, C25–C31.
- Byun B.S. 1984. Seismic parameters for transversely isotropic media. *Geophysics* **49**, 1908–1984.
- Dellinger J.A. and Vernik L. 1994. Do traveltimes in pulse-transmission experiments yield anisotropic group or phase velocities? *Geophysics* **59**, 1774–1779.
- Dewhurst D.N. and Siggins A.F. 2006. Impact of fabric, microcracks, and stress field on shale anisotropy. *Geophysical Journal International* **165**, 135–148.
- King M.S. 1964. *Wave velocities and dynamic elastic moduli of sedimentary rocks*. PhD thesis, University of California, Berkeley, USA.
- Jakobsen M. and Johansen T.A. 2000. Anisotropic approximations for mudstones: a seismic laboratory study. *Geophysics* **65**, 1711–1725.
- Johnston J.E. and Christensen N.I. 1995. Seismic anisotropy of shales. *Journal of Geophysical Research* **100**, 5591–6003.
- Sarout J. and Guéguen Y. 2008. Anisotropy of elastic wave velocities in deformed shales: Part 1-Experimental results. *Geophysics* **73**, D75–D89.
- Sarout J., Molez L., Guéguen Y. and Hoteit N. 2007. Shale dynamic properties and anisotropy under triaxial loading: experimental and theoretical investigations. *Physics and Chemistry of the Earth* **32**, 896–906.
- Sarout J., Esteban L., Delle Piane C., Maney B. and Dewhurst D.N. 2014. Elastic anisotropy of Opalinus Clay under variable saturation and triaxial stress. *Geophysical Journal International* **198**, 1662–1682.
- Sarout J., Piane C.D., Nadri D., Esteban L. and Dewhurst D.N. 2015. A robust experimental determination of Thomsen's  $\delta$ ; parameter. *Geophysics* **80**, A19–A24.
- Sayers C.M. 2004. Seismic anisotropy of shales: What determines the sign of Thomsen's delta parameter? *SEG Expanded Abstracts*.
- Sondergeld C.H. and Rai C.S. 2011. Elastic anisotropy of shales. *The Leading Edge* **30**, 325–331.
- Sondergeld C.H., Rai C.S., Margesson R.W. and Whidden K.J. 2000. Ultrasonic measurement of anisotropy on the Kimmeridge Shale. *SEG Expanded Abstracts*.
- Sone H. 2012. *Mechanical properties of shale gas reservoir rocks and its relation to in-situ stress variation observed in shale gas reservoirs*. PhD thesis, Stanford University, USA.
- Thomsen L. 1986. Weak elastic anisotropy. *Geophysics* **51**, 1954–1966.
- Tsvankin I. 1996. P-wave signatures and notation for transversely isotropic media: an overview. *Geophysics* **61**(2), 467–483.
- Tsvankin I. 2012. *Seismic Signatures and Analysis of Reflection Data in Anisotropic Media*, 3rd edn. Society of Exploration Geophysicists.
- Tsvankin I. and Thomsen L. 1994. Nonhyperbolic reflection moveout in anisotropic media. *Geophysics* **59**(8) 1290–1304.
- Vernik L. and Nur A. 1992. Ultrasonic velocity and anisotropy of hydrocarbon source rocks. *Geophysics* **57**, 727–735.
- Vernik L. and Liu X. 1997. Velocity anisotropy in shales: a petrophysical study. *Geophysics* **62**, 521–532.
- Wang Z. 2002a. Seismic anisotropy in sedimentary rocks, part 1: A single-plug laboratory method. *Geophysics* **67**, 1415–1422.
- Wang Z. 2002b. Seismic anisotropy in sedimentary rocks, part 2: Laboratory data. *Geophysics* **67**, 1423–1430.
- Yan F., Han D.-H. and Yao Q. 2012. Oil shale anisotropy measurement and sensitivity analysis. *SEG Expanded Abstracts*.
- Yan F., Han D.-H. and Yao Q. 2016. Physical constraints on  $c_{13}$  and  $\delta$  for transversely isotropic hydrocarbon source rocks. *Geophysical Prospecting* **64**, 1524–1536.